The systemic administration of an anti-miRNA oligonucleotide encapsulated pH-sensitive liposome results in reduced level of hepatic microRNA-122 in mice

Hiroto Hatakeyama[a], Manami Murata[a], Yusuke Sato[a], Mayumi Takahashi[a], Noriaki Minakawa[b], Akira Matsuda[a], Hideyoshi Harashima[a]

[a] Faculty of Pharmaceutical Sciences, Hokkaido University, Sapporo, Hokkaido, Japan; [b] Graduate School of Pharmaceutical Sciences, The University of Tokushima

* Corresponding author:
Hideyoshi Harashima, PhD
Faculty of Pharmaceutical Sciences
Hokkaido University
Sapporo, Hokkaido, 060-0812, Japan.
Tel.: +81 11 706 3919
Fax: +81 11 706 4879
E-mail: harasima@pharm.hokudai.ac.jp

Keywords: miRNA; antisense oligonucleotide; drug delivery system; liposomes; miR-122

Abstract

Efficient delivery continues to be a challenge in microRNA (miRNA) therapeutics. We utilized a pH-sensitive multifunctional envelope-type nano device (MEND) containing a pH-sensitive lipid YSK05 (YSK05-MEND) to regulate liver specific miRNA-122 (miR-122). Anti-microRNA oligonucleotides including 2'-OMe and phosphorothioate modifications against miR-122 (AMO122) were encapsulated in the YSK05-MEND. Despite the lower uptake, the YSK05-MEND showed a higher activity in liver cancer cells than Lipofectamine2000 (LFN2k) due to efficient endosomal escape. Cytotoxicity was minimal at 100 nM of AMO122 in YSK05-MEND treated cells, but LFN2k showed toxicity at 50 nM. When mice were administrated with free AMO122, it was eliminated via the kidney due to its molecular weight, and lesser amounts were detected in the liver. Conversely, the YSK05-MEND delivered higher amounts of the AMO122 to the liver. Systemic administration of YSK05-MEND induced the knockdown of miR-122 and an increase in target genes in the liver, and a subsequent reduction in plasma cholesterol at a dose of 1 mg AMO/kg while free AMO122 showed no activity at the same dose. The effect of AMO122 delivered by YSK05-MEND persisted for over 2 weeks. These results suggest that YSK05-MEND is a promising system for

delivering AMOs to the liver.

1. Introduction

MicroRNAs (miRNAs) are a class of small non-coding RNAs (~22 nt) that regulate gene expression by binding to the 3'-untranslated region (3'-UTR) of target genes, triggering the degradation of messenger RNA (mRNA) or the inhibition of protein translation [1]. MicroRNA-122 (miR-122) is a conserved liver-specific miRNA that accounts for 70% of the total miRNA population [2] and plays important roles in liver physiology, such as lipid metabolism [3,4], diseases in hepatic virus C (HCV) infections [5] and hepatocellular carcinoma (HCC) [6]. In addition, the expression of miR-122 in other organs such as heart is negligible [7]. Thus, miR-122 is an attractive and selective therapeutic target for the treatment of liver diseases [8].

A number of attempts have been made to induce the specific inhibition of endogenous miRNAs in vivo. Plasmid DNA vectors that express miRNA sponges, which contain multiple tandem miRNA binding sites, have been designed to competitively inhibit miRNA functions in mammalian cells [9]. It was recently reported that the intravenous administration of recombinant adeno associated virus (rAAV) vectors with miRNA tough decoys (TuDs) result in reduced levels of miR-122 and serum cholesterol [10]. Anti-microRNA oligonucleotides (anti-miRs) have been widely employed to inhibit miRNAs, including a variety of nucleoside modifications, such as 2'-O-methyl (2'-OMe), 2'-O-methoxyethyl (2'-MOE), and locked nucleic acid (LNA) was developed in an attempt to enhance binding affinity to target miRNAs with phosphorothioate (PS) linkages to improve nuclease resistance [11]. The systemic injection of these anti-miRs against miR-122 (anti-miR122) into mice resulted in a reduction in cholesterol levels [3,4,12-14]. Miravirsen, an LNA-modified anti-miR122, is currently in phase 2 clinical trials for the treatment of HCV [15].

However, large doses of anti-miR-122 are required to induce the phenotype when the free form of anti-miR-122 is injected due to renal excretion and poor tissue selectivity as well as cellular uptake [16-18]. To overcome these issues, systems that are capable of delivering nucleic acids to a targeted organ are desired [18]. Lipid based nanoparticels have been extensively investigated vehicles for delivering siRNAs, miRNAs, as well as anti-miRs [19-23]. We developed a multifunctional envelope-type nano device (MEND), in which nucleic acids are encapsulated within a lipid envelope [24,25]. We recently synthesized a pH-sensitive cationic lipid, referred to as YSK05 [26]. A MEND composed of YSK05 (YSK05-MEND) showed efficient pH-sensitive fusogenic properties and a higher gene knockdown ability than a commercially available transfection reagent,

Lipofectamine 2000 (LFN2k) in HeLa cells [26]. The systemic administration of YSK05-MEND modified with PEG delivered siRNA to tumor tissue in renal cell carcinoma xenograft mice via the enhanced permeability and retention (EPR) effect and induced the knockdown of approximately 50% of the target gene at a dose of 3 mg/kg body weigh [27]. These findings indicate that YAK05-MEND has the potential for use in nucleic acid delivery both in vitro and in vivo.

In the present study, we report on an investigation of whether the YSK05-MEND could be applicable for use in an anti-miR-122 delivery system to murine liver. We first evaluated the physical properties of the YSK05-MEND encapsulating anti-miR-122 modified with 2'-OMe and PS linkages (AMO122) and its activity in murine hepatoma cells in comparison with LFN2k. For in vivo studies, we compared the activity of systemically administrated YSK05-MEND with free AMO in terms of distribution in the liver and kidney, and the effect of antagonism of target miR-122 on the increase in the expression level of genes that are regulated by miR-122 and the subsequent reduction in plasma cholesterol levels. The findings indicate that the YSK05-MEND has the potential for use in the efficient delivery of AMOs to murine liver.

2. Materials and methods

2.1 Materials

Cholesterol (Chol) was purchased from AVANTI Polar Lipids (Alabaster, AL, USA). 1,2-Dimyristoyl-*sn*-glycerol-methoxypolyethyleneglycol 2000 ether (PEG-DMG) was purchased from NOF Corporation (Tokyo, Japan). YSK05 was synthesized as described previously [26]. Anti-miR against miR-122 (AMO122) (5'-$A_sC_sA_sA_sA_sC_sA_sC_sC_sA_sU_sU_sG_sU_sC_sA_sC_sA_sC_sU_sC_sC_sA$-3') and Cy5-labeled AMO (Cy5-AMO) (5'-Cy5-A_sC_sGAUAAACGGUUGUCUACG$_sU_sC_sA_s$-3') were purchased from Hokkaido System Science Co., Ltd. (Sapporo, Japan) (2'-OMe-modified nucleotides; subscript 's' represents a phosphorothioate linkage). Quant-iT RiboGreen RNA assay was purchased from Molecular Probes (Eugene, OR, USA). MEM alpha, Lipofectamine 2000 (LF2k) and TRIzol were purchased from Invitrogen (Carlsbad, CA, USA). Taqman MicroRNA Reverse Transcription Kit, TaqMan microRNA assay kit, High Capacity RNA-to-cDNA kit, and Fast SYBR Green Master Mix were obtained from Applied Biosystems (Foster City, CA). Amicon Ultra (MWCO 100K) was obtained from Millipore (Bedford, MA, USA). Murine hepatoma Hepa1c1c7 cells obtained from American Type Culture Collection (ATCC, Manassas, VA, USA).

2.2 Preparation of the YSK05-MEND encapsulating AMO122 (AMO122-YSK05-MEND)

The YSK05-MEND was prepared with the pH-sensitive cationic lipid YSK05,

cholesterol and PEG-DMG (molar ratio: 70/30/3) using a *t*-BuOH dilution method. The lipid in 90% (v/v) *t*-BuOH was mixed with AMO122 in 20 mM citrate buffer (pH 4.0) at an AMO/lipid ratio of 0.1 (wt/wt) under strong agitation to a *t*-BuOH concentration of 60% (v/v). The lipid/AMO122 mixture was then added to 20 mM citrate buffer (pH 4.0) under strong agitation to a *t*-BuOH concentration of <12% (v/v). Ultrafiltration was performed using Amicon Ultra for removing *t*-BuOH, replacing external buffer with phosphate buffered saline (PBS, pH 7.4) and concentrating AMO122-YSK05-MEND.

2.3 Characterization of AMO122-YSK05-MEND

The average diameter, polydispersity index (pdi) and zeta-potential of AMO122-YSK05-MEND were determined using a Zetasizer Nano ZS ZEN3600 (MALVERN Instrument, Worchestershire, UK). AMO122 encapsulation efficiency was determined by RiboGreen assay [26]. AMO122-YSK05-MEND was diluted in 10 mM hepes buffer (pH7.4) containing 20 μg/mL dextran sulfate and Ribogreen in the presence or absence of 0.1 w/v% Triton X-100. Fluorescence was measured by a Varioskan Flash (Thermo scientific, Waltham, MA, USA) with λex=500 nm, λem=525 nm. AMO122 concentration was calculated from AMO122 standard curve. AMO122 encapsulation efficiency was calculated by comparing the AMO122 concentration in the presence and absence of Triton X-100. Free AMO122 and AMO122-YSK05-MEND including 1.2 μg AMO122 in the presence and absence of 20 μg/mL dextran sulfate and 0.1 w/v% Triton X-100 were electrophoresed through a 2.5% agarose gel at 100 V for 20 min and then stained with ethidium bromide and visualized under UV light using an Image Quant LAS4000 (GE healthcare, Piscataway, NJ, USA). The pH-sensitivity of AMO122-YSK05-MEND was determined using 6-(*p*-toluidino)-2-naphthalenesulfonic acid (TNS) (Wako, Osaka, Japan) [26]. Thirty μM of lipid of AMO122-YSK05-MEND and 6 μM of TNS were mixed in 200 μL of 20 mM citrate buffer, 20 mM sodium phosphate buffer, or 20 mM Tris-HCl buffer, containing 130 mM NaCl at a pH ranging from 3.0 to 9.0. Fluorescence was measured by a Varioskan Flash with λex=321 nm, λem=447 nm, at 37 °C. The highest fluorescence was relatively assigned value of 1. The curve fitting was accomplished using Sigmaplot 12 (Hulinks, Tokyo, Japan). The pKa values were measured using the fitting curve as the pH giving rise to half-maximal fluorescent intensity.

2.4 in vitro transfection of AMO122 into hepatocytes and RNA isolation

Hepa1c1c7 cells were cultured in cell-culture dishes (Corning, New York, NY, USA) containing MEM alpha supplemented with 10% fetal bovine serum, penicillin (100 U/ml) and streptomycin (100 mg/ml) at 37°C in an atmosphere of 5% CO_2 and 95% humidity. One day prior to the transfection of AMO, 2.5×10^4

Hepa1c1c7 cells were seeded in 6-well plates. AMO122-YSK05-MEND was diluted by MEM alpha supplemented with 10% fetal bovine serum (FBS). The cells were washed by PBS (pH 7.4), then 1.5 ml of MEM alpha containing AMO122-YSK05-MEND at the indicated concentration of AMO122 was added to the wells, followed by incubation at 37°C for 48 hr. LFN2k was used as a control, according to the manufacture's protocol. The cells were washed twice with 1 ml PBS. Total RNA was extracted with TRIzol reagent according to the manufacturer's instructions. To evaluate cytotoxicity, cells were washed twice with PBS at 48 hr, then incubated with 400 μl of Passive Lysis Buffer (Promega, Madison, WI, USA), followed by centrifugation (12000 rpm, 4 °C, 5 min). Protein concentration in the supernatant was determined using BCA Protein Assay Kit (PIERCE, Rockford, IL). Phase-contrast images of the diluted sample were captured using a phase-contrast microscope (CKX41, OLYMPUS, Tokyo, Japan).

2.5 Reverse transcription (RT) and real-time PCR for miRNA and mRNA quantification

Mature miRNA-122 expression was determined using a Taqman MicroRNA Reverse Transcription Kit according to the manufacturer recommended protocols. Briefly, 100 ng of isolated RNA, 0.5 μl of stem-loop RT primer, RT buffer, 1 mM deoxyribonucleoside triphosphate mix, 3.35 units/μl MultiScribe reverse transcriptase, and 0.26 units/μl RNase inhibitor were used in 10 μl RT reactions for 30 min at 16 °C, 30 min at 42 °C, and 5 min at 85 °C. Complementary DNA was then subjected to real-time PCR using a TaqMan™ microRNA assay kit. The 15 μl reaction volume included 5 μl of cDNA (1:60 dilution), 0.75 μl of primer, and 7.5 μl of TaqMan Universal PCR Master Mix reactions was processed in Lightcycler480 system II (Roche) as follows: for 10 min at 95 °C (denaturation) and 40 cycles of 15 sec at 95 °C and 1 min at 60 °C (annealing/extension). miRNA expression was calculated using ΔΔCt method being normalized to small nuclear RNA (snRNA) RNU6B.

For the determination of mRNA, 1.0 μg of isolated RNA was reverse transcribed using a High Capacity RNA-to-cDNA kit according to the manufacturer's instructions as described previously [27]. A quantitative PCR analysis was performed on 20 ng of cDNA using Fast SYBR Green Master Mix and Lightcycler480 system II. All reactions were performed at a volume of 15 μl. The PCR was processed in Lightcycler480 system II as follows: for 20 sec at 95 °C (denaturation) and 40 cycles of 3 sec at 95 °C and 30 sec at 60 °C for 30 sec (annealing/extension). The amount of target gene was calculated using the ΔΔCt method normalized to hypoxanthine phosphoribosyltransferase 1 (*Hprt1*) mRNA. The primers for murine aldolase A (*Aldoa*) were (forward) 5'-GATGGGTCCAGCTTCAAC-3' and (reverse)

5'-GTGCTTTCCTTTCCTAACTCTG-3', branched-chain ketoacid dehydrogenase (*Bckdk*) were (forward) 5'-AGGACCTATGCATGGCTTTG-3' and (reverse) 5'-CCGTAGGTAGACATCCGTG-3', N-myc downstream regulated gene 3 (*Ndrg3*) were (forward) 5'- ATGGGCTACATACCATCTGC-3' and (reverse) 5'-TCTGACTGATTGCTGGTCAC-3' and *Hprt1* were (forward) 5'-CGTGATTAGCGATGATGAAC-3' and (reverse) 5'-GCAAGTCTTTCAGTCCTGTC-3'.

2.6 Determination of cellular uptake of Cy5-AMO encapsulated YSK05-MEND

One day prior to the transfection of Cy5-AMO, Hepa1c1c7 cells were seeded at a density of 1.5 × 10^5 cells per well in 6-well plates (Corning). Cy5-AMO encapsulated YSK05-MEND was diluted with MEM alpha containing 10% FBS, followed by the incubation with cells for 2 hr at 20 nM of AMO. The cells with incubated with LFN2k complexed with Cy5-AMO in MEM alpha for 2 hr at 20 nM of AMO, according to the manufacture's protocol. The cells were washed with 1 ml PBS, and detached by treatment with 0.05% trypsin-PBS. The cells were kept in ice and evaluated on a FACSCalibur flow cytometer (BD Biosciences, San Diego, CA, USA). The results were analyzed using Cell-Quest (BD Biosciences).

2.7 Observation of intracellular trafficking of Cy5-AMO encapsulated MEND

One day prior to transfection, 1.5 × 10^5 Hepa1c1c7 cells were seeded in a 35-mm glass-bottom dish (Iwaki, Osaka, Japan) in 1.5 ml of medium. YSK05-MEND or LFN2k containing Cy5-AMO was added at 100 nM of AMO concentration, followed by incubation at 37°C for 1 hr. The cells were washed twice with 1 ml of PBS, and were then fixed with 4% paraformaldehyde (PFA)-PBS for 10 min. The fixed cells were stained with Hoechst 33342 (Wako, Osaka, Japan) for 10 min. The cells were washed twice with 1 ml of PBS. The cells were added to Krebs Henseleit buffer and images were captured with a FLUOVIEW FV10i confocal microscope (OLYMPUS, Tokyo, Japan) equipped with a × 60 water objective lens.

2.8 in vivo experiments

Female ICR mice (7-8 weeks old) were purchased from Japan SLC (Shizuoka, Japan). One day prior to administration (day -1), blood was collected to determine cholesterol and alanine aminotransferase (ALT) levels. Either free AMO122 or AMO122-YSK05-MEND at a dose of 1 mg/kg AMO122 in a total volume of 10~15 ml/kg was intravenously administered to mice via the tail vein at day 0, 2 and 4. At the indicated times after the administration, blood and liver were collected. Blood sample was centrifuged at 8 *g* at 4°C for 5 min to obtain plasma. To obtain serum, blood samples were stored overnight at 4 °C, followed by centrifugation (10000 rpm, 4 °C, 10 min). Cholesterol in plasma and ALT levels in serum were determined by a Cholesterol *E*-test WAKO and Transaminase CII-test WAKO

(Wako, Osaka, Japan), respectively according to manufacturer recommended protocols. Liver tissue was homogenized in TRIzol using a PreCellys (Bertin Technologies, France). The total RNA in the supernatant was then isolated following the manufacturer's instructions. Target miRNA and mRNA levels were determined as described above. For histological observation, either free Cy5-AMO or YSK05-MEND encapsulating Cy5-AMO was intravenously administered to mice via the tail vein at a dose of 1 mg/kg AMO. At 30 min after administration, each animal was perfused with PBS to remove blood from the liver, which was then collected and fixed in 4% PFA-PBS for 24 hr. The liver was sectioned into 150 μm thick sections using a super microslicer ZERO1 (Dosaka, Kyoto, Japan), and nuclei were stained by Hoechst33342. Images were captured using a Nikon A1 confocal microscope (Nikon, Tokyo, Japan) equipped with a × 60 water objective lens. Kidney tissue stained by Hoechst33342 was imaged by Nikon A1 equipped with a × 40 dry objective lens. The experimental protocols were reviewed and approved by the Hokkaido University Animal Care Committee in accordance with the "Guide for the Care and Use of Laboratory Animals".

2.9 Statistical analysis

Comparisons between multiple treatments were made using one-way analysis of variance (ANOVA), followed by the SNK test. Pair-wise comparisons between treatments were made using a Student's t-test. A P-value of <0.05 was considered as significant difference.

3. Results

3.1 Characterization of the prepared AMO122-YSK05-MEND

The average diameter, pdi and zeta-potential of the AMO122-YSK05-MEND were 71 ± 2 nm, 0.20 ± 0.01 and 3.1 ± 0.5 mV, respectively. The characteristics of empty YSK05-MEND prepared by the same procedure without AMO122 were similar (72 ± 2 d. nm, pdi 0.24 ± 0.02, zeta-potential 7.3 ± 1.2 mV). The recovery and encapsulation efficiency of AMO122 determined with RiboGreen were 91 ± 6 % and 99 ± 1 %, respectively. The encapsulation of AMO122 was also confirmed by electrophoresis (Figure S1a). The apparent pKa of AMO122-YSK05-MEND was determined to be approximately 6.6, indicating that the YSK05-MEND could be converted into a cationic species in early endosomes (Fig. S1b).

3.2 Determination of the in vitro expression of miR-122 targeted genes and cytotoxicity

It has been reported that *Aldoa* is regulated by miR-122, and the inhibition of miR-122 leads to an increase in the expression level of *AldoA* [3,4]. Therefore, we first determined the expression level of *Aldoa* by qRT-PCR after the AMO122-YSK05-MEND treatment in comparison with a commercially available reagent, LFN2k [5,28]. The use of the AMO122-YSK05-MEND caused an increase

in the expression of *Aldoa* in a dose-dependent manner, and the enhancement by AMO122-YSK05-MEND was higher than that for LFN2k/AMO122 complex (717 ± 68 d. nm, pdi 0.43 ± 0.09, zeta-potential 27.1 ± 4.0 mV) (Fig. 1a). Even though the AMO122-YSK05-MEND showed no cytotoxicity up to 100 nM of AMO122, LFN2k showed cytotoxicity at more than 50 nM of AMO, which can be attributed to the potent cationic charge of LFN2k (Fig. 1b and c).

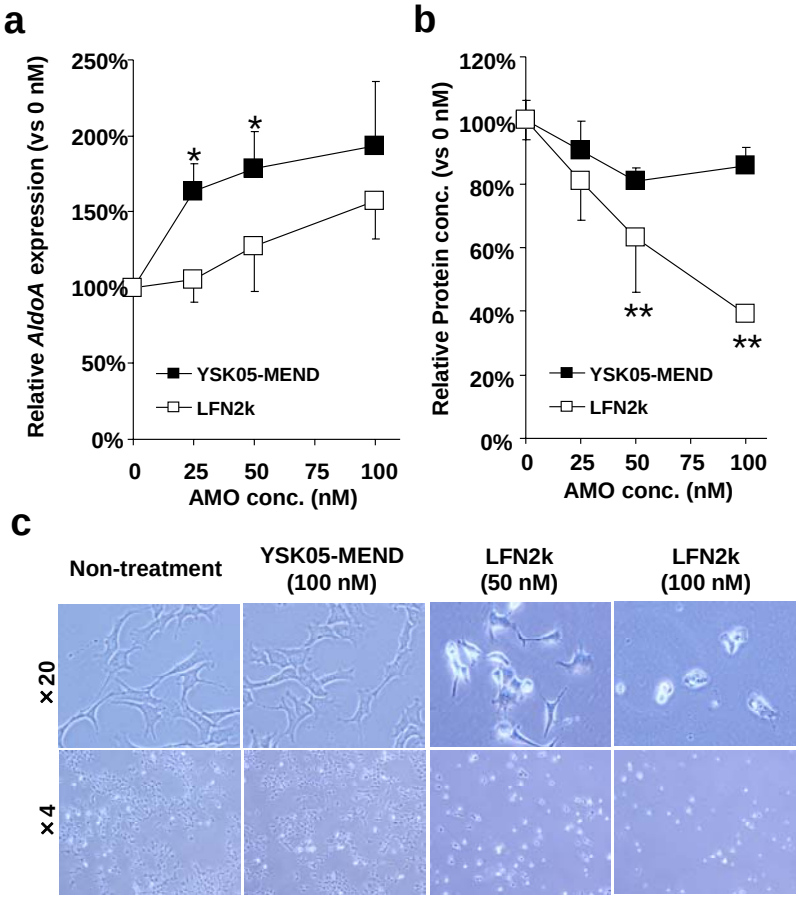

Fig. 1. Expression of miR-122 and *AldoA* and cytotoxicity in vitro

(a) The expression of *Aldo A* in Hepa1c1c7 cells treated with YSK05-MEND or LFN2k at the indicated AMO122 concentrations was evaluated by qRT-PCR. The expression of *AldoA* was normalized to *Hprt1*. Data are represented as relative expression levels to that treated with PBS (0 nM). The mean ± SD (n=3). (b) Protein levels were determined after treatment with YSK05-MEND or LFN2k. Data are represented relative values to that treated with PBS (0 nM).The Mean ± SD (n=3). *P<0.05, **P<0.01 YSK05-MEND v.s. LFN2k at indicated AMO concentrations.

The uptake amount of Cy5-labeled AMO (Cy5-AMO) formulated in the YSK05-MEND and LFN2k was assessed by flow cytometery. LFN2k. A heterogeneous cellular uptake of Cy5-AMO was observed in the case of LFN2k. On the other hand, Cy5-AMO was homogenously taken up by cells that had been treated with YSK05-MEND (Fig. 2a). Despite the higher activity (Fig. 1a), the relative mean fluorescent intensity of the YSK05-MEND treated cells was around 2 fold less than that for LFN2k (Fig. 2b). Intracellular observations indicated that aggregated forms of Cy5-AMO were produced when LFN2k was used, but diffused pattern was found in the case of YSK05-MEND (Fig. 2c). These findings suggest that Cy5-AMOs formulated in LFN2k becomes trapped in endosomes/lysosomes or in vesicular compartments. On the other hand, Cy5-AMOs encapsulated in

YSK05-MEND was able to efficiently escape from endosomes. These results indicate that a pH-sensitive MEND composed of YSK05 induced the efficient inhibition of miRNA by delivering AMO to the cytosol and subsequently increasing the expression of the target genes.

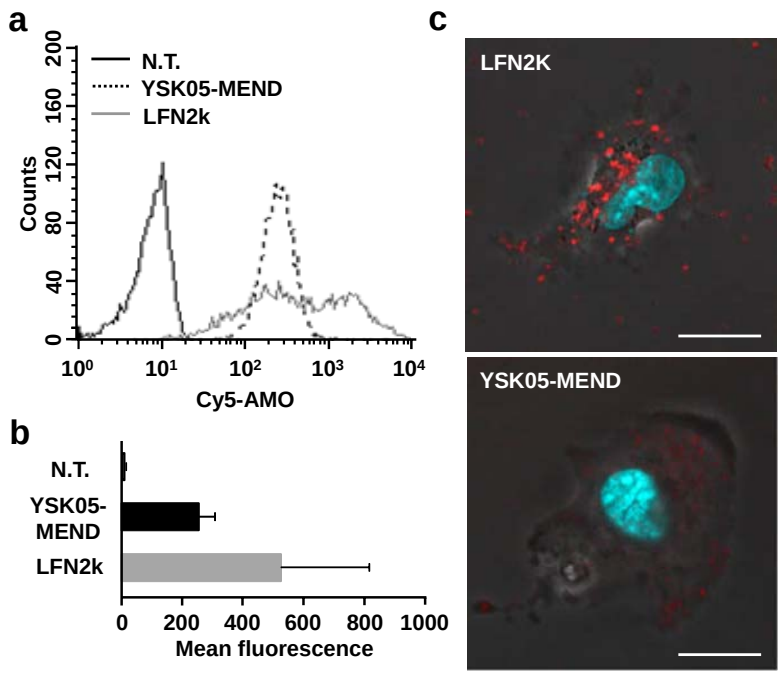

Fig. 2. Cellular uptake and intracellular distribution of Cy5-AMO. (a) The uptake of Cy5-AMO formulated in the YSK05-MEND and LFN2k were determined by a flow cytometery, after a 2 hr incubation at 20 nM AMO. (b) Bars represent average fluorescence obtained by flow cytometric analysis (n=3). N.T.: Non-treatment. (c) The intracellular pattern of Cy5-AMO (red) formulated in YSK05-MEND and LFN2k was observed by a confocal laser scanning microscope after the incubation for 2 hr at 80 nM AMO. Nuclei were stained with Hoechst 33342 prior to observation (cyan). Scale bars indicate 20 μm.

3.3 In vivo evaluation of AMO encapsulated YSK05-MEND

We next evaluated the in vivo efficacy of the AMO122-YSK05-MEND in the liver. It is known that LFN2k cannot be used in vivo, and therefore, chemically modified anti-miRs are largely administered as a free form in in vivo studies [3,4,12-14]. Therefore, we used free AMO122 as a control in the in vivo studies. To observe the distribution of AMOs, mice were administered with the YSK05-MEND encapsulating Cy5-AMO via the tail vein. After 30 min, nuclear stained liver sections were prepared and observed by confocal laser scanning microscopy. As shown in Fig. 3, the administration of the YSK05-MEND resulted in a higher fluorescent signal of Cy5-AMO in the liver as compared to that of free Cy5-AMO. Conversely, the free Cy5-AMO accumulated at higher levels in the kidney than the YSK05-MEND because the free Cy5-AMO was excreted via the kidney due to its molecular weight.

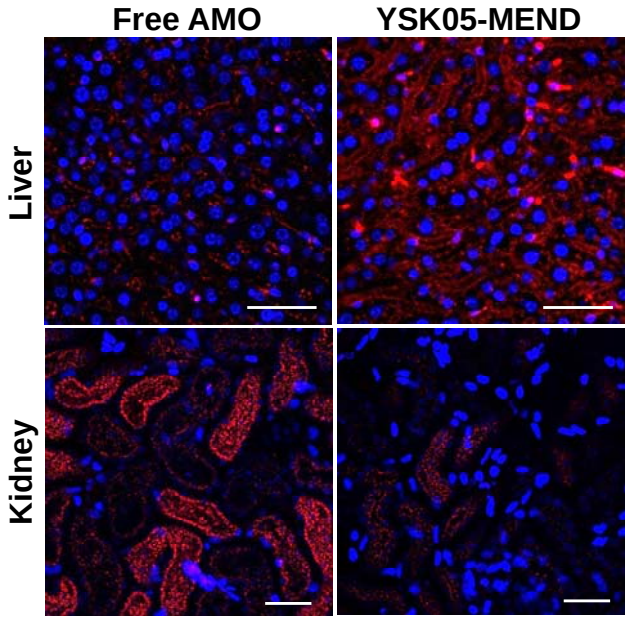

Fig. 3. Histological observations of Cy5-AMO in the liver and kidney. Mice were injected via the tail vein with either free Cy5-AMO or Cy5-AMO encapsulated in the YSK05-MEND (red). Liver and kidney were collected 30 min later. Nuclei in liver and kidney were stained with Hoechst33342 (blue). Images were captured by a CLSM. Scale bars are 50 μm.

We evaluated the knockdown of miR-122 in the liver. Either free AMO122, AMO122-YSK05-MEND or empty YSK05-MEND was successively administered three times at a dose of 1 mg AMO122/kg. Even though the administration of free AMO122 resulted in an approximately 30% knockdown of miR-122, the AMO122-YSK05-MEND significantly reduced the expression of miR-122 as compared to free AMO122 as well as the empty YSK05-MEND at 48 hr after the last administration (day 6) (Fig. 4a). The expression levels of genes that are regulated by miR-122 were determined. YSK05-MEND enhanced the expression of *AldoA*, *Bckdk* and *Ndrg3*, while no increase in the expression of these genes was found in the case of free AMO122 (Fig.4b). These alternations were not observed when YSK05-MEND encapsulating AMO against miR-10b (AMO10b) was used (Fig. S2). It was reported that miR-122 is a key regulator of cholesterol, and the inhibition of miR-122 resulted in a decrease in plasma cholesterol levels [3,4]. Hence, plasma cholesterol levels were measured. Plasma cholesterol levels were decreased by around 30% only by treatment with the AMO122-YSK05-MEND at 48 hr after the last injection (day 6) (Fig. 4c).

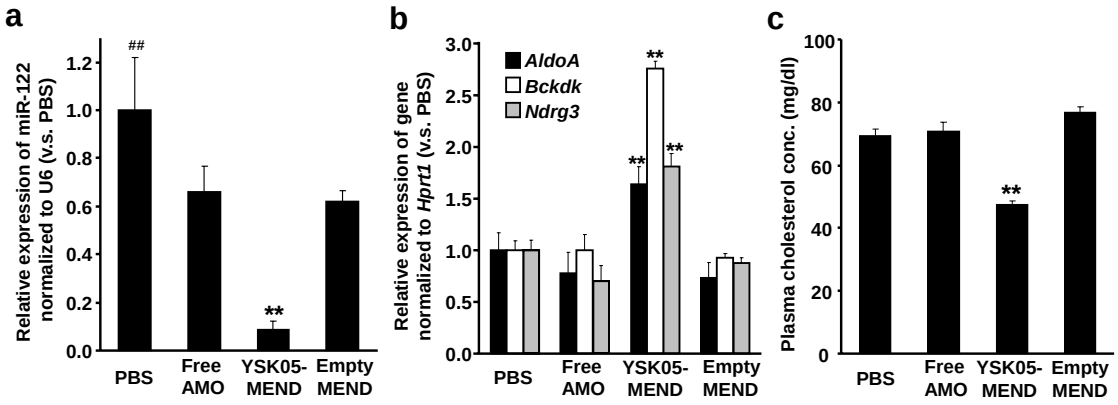

Fig. 4. Expression of miR-122 and target genes in the liver and cholesterol levels in plasma. Mice were injected at day 0, 2 and 4 via the tail vein with either PBS, free AMO122 (1 mg AMO/kg), AMO122-YSK05-MEND (1 mg AMO/kg) or empty YSK05-MEND. At 48 hr after the last injection (day 6), the expression of (a) miR-122 and (b) *AldoA*, *Bckdk* and *Ndrg3* in liver and (c) plasma cholesterol level were determined (the mean ± SD, n=4). **P<0.01 YSK05-MEND v.s. the others. $^{\#\#}$P<0.01 PBS v.s. the others.

We further monitored the expression of miR-122 and its target genes at days 6, 12 and 25, as well as plasma cholesterol levels until day 25 after the AMO122-YSK05-MEND treatment and compared the findings to that of PBS to estimate the durability of AMO122-YSK05-MEND. The knockdown of miR-122 and enhancement of the genes by AMO122-YSK05-MEND continued until day 12 (Fig. 5a and d). The significant decline in plasma cholesterol levels continued until day 18 compared to the control that was treated with PBS (Fig. 5c). On the other hand, no significant difference in body weight was observed over the 25 days (Fig. 5d). Because liposomal systems mainly accumulate in the liver, hepatotoxicity was evaluated. The findings showed that no increase in serum ALT levels occurred at 48 hr after the last injection of AMO122-YSK05-MEND (Fig. 5e).

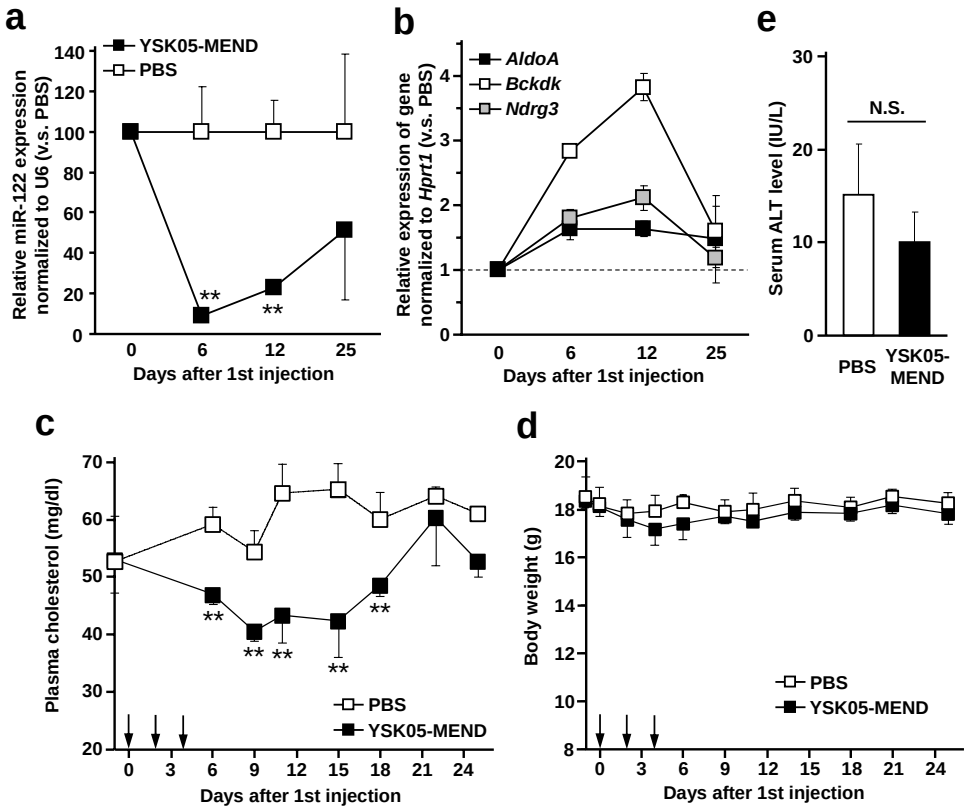

Fig. 5. Long-term observation of the expression level of miR-122 and target genes in the liver and plasma cholesterol levels. Mice were injected via the tail vein with either PBS or AMO122-YSK05-MEND at day 0, 2 and 4. (a, b) The expression of miR-122 (a) and target genes (b) in liver was determined at day 6, 12

and 25. (c, d) The cholesterol level in plasma (c) and body weight (d) were monitored over 25 days. Arrows indicate the injections at day 0, 2 and 4. (e) Serum ALT was determined at day 6. Data are represented as the mean ± SD (n=4). **P<0.01 v.s. PBS-treatment at indicated time points. N.S.: Not significant difference.

4. Discussion

MiRNAs have emerged as important post-transcriptional regulators of gene expression in biological processes [1]. Loss of function studies using miRNA gene knockout techniques are frequently utilized to explore the functions of miRNAs [11,29]. However, the generation of genetic knockouts is difficult, complicating and time consuming. A widely employed approach in loss-of-function studies is to use chemically modified anti-miRs [3-5,12-14], and LNA-modified anti-miR has some potential for clinical use in the treatment of HCV infections [15]. For a successful anti-miRNA therapy using anti-miRs, the anti-miRs must be delivered to the final destination, i.e. the cytoplasm of the target cell. Even though a variety of chemical modifications have been reported to improve nuclease resistance and binding affinity to miRNAs, the delivery of anti-miRs to target organs and the cytoplasm in target cells continues to be a significant challenge. Significant efforts have been devoted to exploring novel delivery strategies, and liposomal nanoparticles represent one of the advanced systems for the delivery of nucleic acids [18-23]. We developed a pH-sensitive MEND with a pH-sensitive lipid, YSK05 (YSK05-MEND), which has neutral surface at physiological pH, but develops a cationic surface in an acidic compartment such as endosomes/lysosomes [26,27]. In the present study, we attempted to utilize YSK05-MEND to deliver an anti-miR modified with 2'-OMe and PS linkage (AMO) to liver.

We first compared the YSK05-MEND with a commercially available reagent, LFN2k in murine hepatoma Hepa1c1c7 cells (Figs.1 and 2). Despite its neutral surface charge, the AMO122-YSK05-MEND showed activity in the cultured cells (Fig. 1a). It was reported that neutral liposomes absorb apolipoprotein E (apoE) in the circulation, which enhances the uptake of the liposomes by hepatocytes via low-density lipoprotein (LDL) receptors (LDLRs) that are expressed on the surface of hepatocytes [30,31]. Since Hepa1c1c7 cells express LDLR (Fig. S3), it is likely that the YSK05-MEND was taken up by the cells via the interaction with LDLRs following the association of YSK05-MEND with apoE in the serum-containing culture media. On the other hand, a lipoplex composed of the cationic liposomal reagent LFN2k and AMO is taken up via endocytosis following its association with anionic molecules on the cell surface [32,33]. Despite the about 2 fold higher uptake of Cy5-AMO (Fig. 2b), the efficiency of AMO122 in LFN2k was inferior to that for the YSK05-MEND (Fig. 1a). It appears that the

Cy5-AMOs delivered by LFN2k become trapped in endosomes/lysosomes or vesicular compartments because Cy5-AMOs become aggregated, as evidence by the appearance of a punctuate pattern (Fig. 2c). This suggest that LFN2k cannot escape efficiently from endosomal/lysosomal compartments. In contrast, the pattern for the signals for Cy5-AMO delivered by the YSK05-MEND were defused. With an apparent pKa of about 6.6 (Fig. S1b), the AMO122-YSK05-MEND becomes a cationic species in response to the acidic environment of early endosomes, which triggers membrane fusion with the endosomal membrane. Our previous study showed that the fusion activity of YSK05-MEND was dramatically superior to that of a MEND composed of a conventional cationic lipid, such as DOTAP [26]. This allows the AMOs encapsulated in the YSK05-MEND to efficiently escape from endosomes into the cytosol, which could result in the diffuse Cy5-AMO signals. For the reasons stated above, the pH-sensitive YSK05-MEND showed a higher activity than LFN2k. Furthermore, cytotoxicity was observed only in the LFN2k treated cells (Fig. 1b and c). Previous studies have reported that cationic lipids induce cytotoxicity including cell shrinking, thus reduced the level of mitosis and vacuolization of the cytoplasm [34]. Therefore, the neutral characteristics of the YSK05-MEND in the cytosol also contribute to the reduced cytotoxicity.

For in vivo evaluation, the YSK05-MEND encapsulating AMO122 was tested in comparison with free AMO122 because LFN2k cannot be applied to systemic use, and chemically modified anti-miRs are largely used as the free form to regulate target miR-122 in liver [11]. Previous in vivo studies using mice reported that an effective miR-122 knockdown involves the use of a total intravenous dose of 240 mg/kg (80 mg/kg three times) of cholesterol-conjugated 2'-O-Me antagomir [3], total intraperitoneal doses of 100-600 mg/kg (12.5-75 mg/kg twice weekly for four weeks) of 2'-MOE oligonucleotides [4], a total intravenous dose of 75 mg/kg LNA-antimiR (25 mg/kg three consecutive days) [12], and a total intravenous dose of 60 mg/kg (20 mg/kg three times) of tiny LNA [14], which resulted in the lowering of a plasma cholesterol phenotype. These findings indicate that high doses are required to exert their function when anti-miRs are used as a free form, which can be attributed to the pharmacokinetic properties of anti-miRs. Small molecules having a molecular weight of < 50 kDa or a diameter < 6-8 nm are cleared from the systemic circulation by glomerular filtration in the kidney [16,17]. Since the molecular weight of anti-miRs is generally around 8 kDa, systemically administrated anti-miRs are largely eliminated via the kidney, which results the limited availability of anti-miR in hepatocytes and the need for high doses. It was reported that siRNA delivered by a stable nucleic acids lipid nanoparticle (SNALP) induced the knockdown of a target gene in the liver at lower doses (0.1~1

mg/kg) than that for a cholesterol conjugated siRNA (50~100 mg/kg) [19]. This suggests that drug delivery technologies could alter the pharmacokinetic properties of nucleic acids and permit their function to be exerted with a lower dose of nucleic acid. We evaluated whether YSK05-MEND was a valid route for the systemic delivery of AMO122 to the liver in comparison with the administration of free AMO122.

Prior to functional analysis, the distribution of Cy5-AMOs in the liver and kidney was evaluated. Systemically administrated free Cy5-AMO was found in the kidney and not in the liver (Fig. 3). In contrast, Cy5-AMO encapsulated in YSK05-MEND was mainly delivered to the liver with decreasing the accumulation of Cy5-AMO in the kidney compared to that for free Cy5-AMO because the diameter (about 70 nm) prevented the YSK05-MEND from being cleared by the renal route. As mentioned above, neutral liposomes acquire ApoE in the circulation, followed by hepatic uptake via LDLRs that are expressed on the surface of hepatocytes [30,31]. It was also reported that the average diameter of sinusoidal fenestrae in C57CL/B mice is 141 nm [35]. Being 70 nm in average diameter, the YSK05-MEND could pass through fenestrae and access hepatocytes. Therefore, it is reasonable to suppose that the YSK05-MEND was taken up by hepatocytes mediated by the association of ApoE with LDL receptors, which resulted in an enhanced delivery of AMOs to the livers in mice after systemic administration.

The three intravenous injections of AMO122-YSK05-MEND at a dose of 1 mg AMO/kg led to the efficient inhibition of miR-122 in the liver and an increase in *AldoA*, *Bckdk* and *Ndrg3* (Fig. 4a and b), while the treatment of free AMO122, the empty YSK05-MEND and the YSK05-MEND encapsulating AMO10b resulted in negligible change (Fig. S2). This suggests that the inhibition of miR-122 and subsequent increment in target genes can be attributed to the antagonism of miR-122 with AMO122. The inhibition persisted until at least day 12 (Fig. 5a, b and c). The durability of AMO122 delivered via the YSK05-MEND was consistent with a previous report [12]. It is well known that chemical modification including 2'-O-Me and phosphorothioate linkages in oligonucleotides improve resistance to nucleases and the binding affinity to the target sequence compared to unmodified ones, which enhances and prolongs their effect [3,11,36,37]. It was suggested that chemically modified AMO122 remained intact for approximately 2 weeks in hepatocytes. However, in addition to the stability of AMO122, the half-lives of miR122, target genes, and cholesterol could also affect the time-dependent change, further study will be required to reveal the correct mechanism responsible for the inhibition of miR-122 by AMO122. In addition, the AMO122-YSK05-MEND caused no alterations in body weight or serum markers of liver toxicity, ALT (Fig.

5d and e), indicating that the YSK05-MEND is not associated with any serious acute toxicity.

5. Conclusion

In the present study, we demonstrated the delivery of AMO to hepatocytes by the intravenous administration of AMOs encapsulated in a pH-sensitive YSK05-MEND. The use of the AMO122-YSK05-MEND resulted in the efficient enhancement of *AldoA* in vitro owing to its ability to escape from endosomes in comparison with LFN2k. Systemically administrated Cy5-AMO formulated in YSK05-MEND was delivered to the liver rather than kidney, whereas free Cy5-AMO mainly accumulated in the kidney due to its low molecular weight. Antagonism of the target miR-122 and the subsequent increase in the expression level of genes in the liver and the decrease in plasma cholesterol levels were induced by AMO122-YSK05-MEND at a total dose of 3 mg AMO/kg, while a comparable dose of free AMO122 had no effect. Even though anti-miRs are utilized in the free form for regulation of miRNA in clinical procedures, high doses are required. The present study demonstrates that the use of drug delivery technologies presents a practical and valuable alternative to anti-miRNA therapeutics. Collectively, YSK05-MEND represents a promising system for use in the in vivo delivery of AMO to the liver.

Acknowledgment

This work was supported in part by a Grant-in-Aid for Scientific Research on Innovative Area “Nanomedicine Molecular Science” (No. 2306), a Grant-in-Aid for Scientific Research (grant No. 23249008) from the Ministry of Education, Culture, Sports, Science and Technology (MEXT) in Japan and the Special Education and Research Expenses of MEXT. The authors also with to thank De. Milton S. Feather for his helpful advice in writing the English manuscript.

References

[1] V. Ambros, The functions of animal microRNAs, Nature 431 (2004) 350-355.

[2] M. Lagos-Quintana, R. Rauhut, A. Yalcin, J. Meyer, W. Lendeckel, T. Tuschl, Identification of tissue-specific microRNAs from mouse, Curr. Biol. 12 (2002) 735-739.

[3] J. Krützfeldt, N. Rajewsky, R. Braich, K.G. Rajeev, T. Tuschl, M. Manoharan, M. Stoffel. Silencing of microRNAs in vivo with 'antagomirs', Nature 438 (2005) 685-689.

[4] avis, S.F. Murray, X.X. Yu, S.K. Pandey, M. Pear, L. Watts, S.L. Booten, M. Graham, R. McKay, A. Subramaniam, S. Propp, B.A. Lollo, S. Freier, C.F. Bennett, S. Bhanot, B.P. Monia. miR-122 regulation of lipid metabolism revealed by in vivo antisense targeting, Cell Metab. 3 (2006) 87－98.

[5] C.L. Jopling, M. Yi, A.M. Lancaster, S.M. Lemon, P. Sarnow, Modulation of hepatitis C virus RNA abundance by a liver-specific MicroRNA, Science 309 (2005) 1577-1581.

[6] C. Coulouarn, V.M. Factor, J.B. Andersen, M.E. Durkin, S.S. Thorgeirsson, Loss of miR-122 expression in liver cancer correlates with suppression of the hepatic phenotype and gain of metastatic properties, Oncogene 28 (2009) 3526-3536.

[7] X. Tang, J. Gal, X. Zhuang, W. Wang, H. Zhu, G. Tang, A simple array platform for microRNA analysis and its application in mouse tissues, RNA 12 (2007) 1803-1822.

[8] A.P. Lewis, C.L. Jopling. Regulation and biological function of the liver-specific miR-122, Biochem. Soc. Trans. 38 (2010) 1553-1557.

[9] M.S. Ebert, J.R. Neilson, P.A. Sharp, MicroRNA sponges: competitive inhibitors of small RNAs in mammalian cells. Nat. Methods 4 (2007) 721-726.

[10] J. Xie, S.L. Ameres, R. Friedline, J.H. Hung, Y. Zhang, Q. Xie, L. Zhong, Q. Su, R. He, M. Li, H. Li, X Mu, H. Zhang, J.A. Broderick, J.K. Kim, Z. Weng, T.R. Flotte, P.D. Zamore, G. Gao, Long-term, efficient inhibition of microRNRNA function in mice using rAAV vectors, Nat. Methods 9 (2012) 403-409.

[11] J. Stenvang, A. Petri, M. Lindow, S. Obad, S.J. Kauppinen, Inhibition of microRNA function by antimiR oligonucleotides, Silence 3:1 (2012).

[12] J. Elmén, M. Lindow, A. Silahtaroglu, M. Bak, M. Christensen, A. Lind-Thomsen, M. Hedtjärn, J.B. Hansen, H.F. Hansen, E.M. Straarup, K. McCullagh, P. Kearney, S. Kauppinen. Antagonism of microRNA-122 in mice by systemically administered LNA-antimiR leads to up-regulation of a large set of predicted target mRNAs in the liver, Nucleic Acids Res. 36 (2008) 1153-1162.

[13] J. Elmén, M. Lindow, S. Schütz, M. Lawrence, A. Petri, S. Obad, M. Lindholm, M. Hedtjärn, H.F. Hansen, U. Berger, S. Gullans, P. Kearney, P. Sarnow, E.M. Straarup, S. Kauppinen. LNA-mediated microRNA silencing in non-human primates, Nature 452 (2008) 896-899.

[14] S. Obad, C.O. dos Santos, A. Petri, M. Heidenblad, O. Broom, C. Ruse, C. Fu, M. Lindow, J. Stenvang, E.M. Straarup, H.F. Hansen, T. Koch, D. Pappin, G.J. Hannon, S. Kauppinen, Silencing of microRNA families by seed-targeting tiny LNAs. Nat. Genet. 43 (2011) 37378.

[15] H.L. Janssen, H.W. Reesink, F.J. Lawitz, S. Zeuzem, M. Rodriguez-Torres, K. Patel, A.J. van der Meer, A.K. Patick, A. Chen, Y. Zhou, R. Persson, B.D. King, S. Kauppinen, A.A. Levin, M.R. Hodges, Treatment of HCV infection by targeting microRNA, N. Engl. J. Med. 368 (2013) 1685-1694.

[16] B. Haraldsson, J. Nyström, W.M. Deen, Properties of the glomerular barrier and mechanisms of proteinuria. Physiol Rev, 88 (2008) 451-487.

[17] R.M. Bukowski, C. Tendler, D. Cutler, E. Rose, M.M. Laughlin, P. Statkevich, Treating cancer with PEG Intron: pharmacokinetic profile and dosing guidelines for an improved interferon-alpha-2b formulation, Cancer 95 (2002) 389-396.

[18] C.V. Pecot, G.A. Calin, R.L. Coleman, G. Lopez-Berestein, A.K. Sood, RNA interference in the clinic: challenges and future directions, Nat Rev Cancer 11 (2011) 59-67.

[19] T.S. Zimmermann, A.C. Lee, A. Akinc, B. Bramlage, D. Bumcrot, M.N. Fedoruk, et al, RNAi-mediated gene silencing in non-human primates, Nature 441 (2006) 111-114.

[20] S.C. Semple, A. Akinc, J. Chen, AP. Sandhu, B.L. Mui, C.K. Cho, D.W. Sah, D. Stebbing, E.J. Crosley, E. Yaworski, I.M. Hafez, J.R. Dorkin, J. Qin, K. Lam, K.G. Rajeev, K.F. Wong, L.B. Jeffs, L. Nechev, M.L. Eisenhardt, M. Jayaraman, M. Kazem, M.A. Maier, M. Srinivasulu, M.J. Weinstein, Q. Chen, R. Alvarez, S.A. Barros, S. De, S.K. Klimuk, T. Borland, V. Kosovrasti, W.L. Cantley, Y.K. Tam, M. Manoharan, M.A. Ciufolini, M.A. Tracy, A. de Fougerolles, I. MacLachlan, P.R. Cullis, T.D. Madden, M.J. Hope, Rational design of cationic lipids for siRNA delivery, Nat. Biotechnol. 28 (2010) 172-176.

[21] M. Jayaraman, S.M. Ansell, B.L. Mui, Y.K. Tam, J. Chen, X. Du, D. Butler, L. Eltepu, S. Matsuda, J.K. Narayanannair, K.G. Rajeev, I.M. Hafez, A. Akinc, M.A. Maier, M.A. Tracy, P.R. Cullis, T.D. Madden, M. Manoharan, M.J. Hope, Maximizing the potency of siRNA lipid nanoparticles for hepatic gene silencing in vivo, Angew. Chem. Int. Ed. Engl. 51 (2012) 8529-8533.

[22] D. Yang, Y. Sun, L. Hu, H. Zheng, P. Ji, C.V. Pecot, Y. Zhao, S. Reynolds, H. Cheng, R. Rupaimoole, D. Cogdell, M. Nykter, R. Broaddus, C. Rodriguez-Aguayo, G. Lopez-Berestein, J. Liu, I. Shmulevich, A.K. Sood, K. Chen, W. Zhang, Integrated analyses identify a master microRNA regulatory network for the mesenchymal subtype in serous ovarian cancer, Cancer Cell 23 (2013) 186-199.

[23] S. Anand, B.K. Majeti, L.M. Acevedo, E.A. Murphy, R. Mukthavaram, L. Scheppke, M. Huang, D.J. Shields, J.N. Lindquist, P.E. Lapinski, P.D. King, S.M. Weis, D.A. Cheresh, MicroRNA-132-mediated loss of p120RasGAP activates the endothelium to facilitate pathological angiogenesis, Nat. Med. 16 (2010) 909-914.

[24] H. Hatakeyama, H. Akita, H. Harashima, A multifunctional envelope type nano device (MEND) for gene delivery to tumours based on the EPR effect: a strategy for overcoming the PEG dilemma, Adv. Drug Deliv. Rev. 63 (2011)

152–160.H. Hatakeyama, H. Akita, H. Harashima, Adv. Drug Deliv. Rev. (2011) 152-160.

[25] T. Nakamura, H. Akita, Y. Yamada, H. Hatakeyama, H. Harashima, A multifunctional envelope-type nanodevice for use in nanomedicine: concept and applications, Acc. Chem. Res. 45 (2012) 1113-1121.

[26] Y. Sato, H. Hatakeyama, Y. Sakurai, M. Hyodo, H. Akita, H. Harashima, A pH-sensitive cationic lipid facilitates the delivery of liposomal siRNA and gene silencing activity in vitro and in vivo, J. Control. Release 163 (2012) 267-276.

[27] Y. Sakurai, H. Hatakeyama, Y. Sato, M. Hyodo, H. Akita, H. Harashima, Gene silencing via RNAi and siRNA quantification in tumor tissue using MEND, a liposomal siRNA delivery system. Mol. Ther. 21 (2013) 1195-1203.

[28] S. Davis, B. Lollo, S. Freier, C. Esau, Improved targeting of miRNA with antisense oligonucleotides, Nucleic Acids Res. 34 (2006) 2294-2304.

[29] S.H. Hsu, B. Wang, J. Kota, J. Yu, S. Costinean, H. Kutay, L. Yu, S. Bai, K. La Perle, R.R. Chivukula, H. Mao, M. Wei, K.R. Clark, J.R. Mendell, M.A. Caligiuri, S.T. Jacob, J.T. Mendell, K. Ghoshal, Essential metabolic, anti-inflammatory, and anti-tumorigenic functions of miR-122 in liver, J. Clin. Invest. 122 (2012) 2871-2883.

[30] X. Yan, F. Kuipers, L.M. Havekes, R. Havinga, B. Dontje, K. Poelstra, G.L. Scherphof, J.A. Kamps, The role of apolipoprotein E in the elimination of liposomes from blood by hepatocytes in the mouse, Biochem. Biophys. Res. Commun. 328 (2005) 57-62.

[31] A. Akinc, W. Querbes, S. De, J. Qin, M. Frank-Kamenetsky, K.N. Jayaprakash, M. Jayaraman, K.G. Rajeev, W.L. Cantley, JR. Dorkin, J.S. Butler, L. Qin, T. Racie, A. Sprague, E. Fava, A. Zeigerer, M.J. Hope, M. Zerial, D.W. Sah, K. Fitzgerald, M.A. Tracy, M. Manoharan, V. Koteliansky, A.D. Fougerolles, M.A. Maier, Targeted delivery of RNAi therapeutics with endogenous and exogenous ligand-based mechanisms, Mol. Ther. 18 (2010) 1357-1364.

[32] K.A. Mislick, J.D. Baldeschwieler, Evidence for the role of proteoglycans in cation-mediated gene transfer, Proc. Natl. Acad. Sci. U.S.A. 93 (1996) 12349-12354.

[33] L.C. Mounkes, W. Zhong, G. Cipres-Palacin, T.D. Heath, R.J. Debs, Proteoglycans mediate cationic liposome-DNA complex-based gene delivery in vitro and in vivo. J. Biol. Chem., 273, 26164-26170 (1998).

[34] H. Lv, S. Zhang, B. Wang, S. Cui, J. Yan, Toxicity of cationic lipids and cationic polymers in gene deliver, J. Control. Release 114 (2006) 100-109.

[35] J. Snoeys, J. Lievens, E. Wisse, F. Jacobs, H. Duimel, D. Collen, P. Frederik, B. D. Geest, Species differences in transgene DNA uptake in

hepatocytes after adenoviral transfer correlate with the size of endothelial fenestrae, Gene Ther. 14 (2007) 604-612.

[36] J. Krützfeldt, S. Kuwajima, R. Braich, K.G. Rajeev, J. Pena, T. Tuschl, M. Manoharan, M. Stoffel, Specificity, duplex degradation and subcellular localization of antagomir, Nucleic Acids Res. 35 (2007) 2885-2892.

[37] M. Takahashi, C. Nagai, H. Hatakeyama, N. Minakawa, H. Harashima, A. Matsuda, Intracellular stability of 2'-OMe-4'-thioribonucleoside modified siRNA leads to long-term RNAi effect, Nucleic Acids Res. 40 (2012) 5787-5793.

Figure caption

Fig. 1. Expression of miR-122 and *AldoA* and cytotoxicity in vitro. (a) The expression of *Aldo A* in Hepa1c1c7 cells treated with YSK05-MEND or LFN2k at the indicated AMO122 concentrations was evaluated by qRT-PCR. The expression of *AldoA* was normalized to *Hprt1*. Data are represented as relative expression levels to that treated with PBS (0 nM). The mean ± SD (n=3). (b) Protein levels were determined after treatment with YSK05-MEND or LFN2k. Data are represented relative values to that treated with PBS (0 nM).The Mean ± SD (n=3). *P<0.05, **P<0.01 YSK05-MEND v.s. LFN2k at indicated AMO concentrations.

Fig. 2. Cellular uptake and intracellular distribution of Cy5-AMO. (a) The uptake of Cy5-AMO formulated in the YSK05-MEND and LFN2k were determined by a flow cytometery, after a 2 hr incubation at 20 nM AMO. (b) Bars represent average fluorescence obtained by flow cytometric analysis (n=3). N.T.: Non-treatment. (c) The intracellular pattern of Cy5-AMO (red) formulated in YSK05-MEND and LFN2k was observed by a confocal laser scanning microscope after the incubation for 2 hr at 80 nM AMO. Nuclei were stained with Hoechst 33342 prior to observation (cyan). Scale bars indicate 20 μm.

Fig. 3. Histological observations of Cy5-AMO in the liver and kidney. Mice were injected via the tail vein with either free Cy5-AMO or Cy5-AMO encapsulated in the YSK05-MEND (red). Liver and kidney were collected 30 min later. Nuclei in liver and kidney were stained with Hoechst33342 (blue). Images were captured by a CLSM. Scale bars are 50 μm.

Fig. 4. Expression of miR-122 and target genes in the liver and cholesterol levels in plasma. Mice were injected at day 0, 2 and 4 via the tail vein with either PBS, free AMO122 (1 mg AMO/kg), AMO122-YSK05-MEND (1 mg AMO/kg) or empty YSK05-MEND. At 48 hr after the last injection (day 6), the expression of (a) miR-122 and (b) *AldoA*, *Bckdk* and *Ndrg3* in liver and (c) plasma cholesterol level were determined (the mean ± SD, n=4). **P<0.01 YSK05-MEND v.s. the others. ##P<0.01 PBS v.s. the others

Fig. 5. Long-term observation of the expression level of miR-122 and target genes in the liver and plasma cholesterol levels. Mice were injected via the tail vein with either PBS or AMO122-YSK05-MEND at day 0, 2 and 4. (a, b) The expression of miR-122 (a) and target genes (b) in liver was determined at day 6, 12 and 25. (c, d) The cholesterol level in plasma (c) and body weight (d) were monitored over 25 days. Arrows indicate the injections at day 0, 2 and 4. (e) Serum ALT was determined at day 6. Data are represented as the mean ± SD (n=4). **P<0.01 v.s. PBS-treatment at indicated time points. N.S.: Not significant difference.